

Effects of Catalyst Acidity and HZSM-5 Channel Volume on Polypropylene Cracking

DARREL L. NEGELEIN, RONG LIN, ROBERT L. WHITE

Department of Chemistry and Biochemistry, University of Oklahoma, Norman, Oklahoma 73019

Received 17 February 1997; accepted 24 June 1997

ABSTRACT: Effects of catalyst acidity and the restricted reaction volume afforded by HZSM-5 on the catalytic cracking of polypropylene are described. Polypropylene cracking by silica–alumina and HZSM-5 catalysts yields olefins as primary volatile products. In addition, HZSM-5 channels restrict carbenium ion rearrangements and facilitate formation of significant amounts of propene and alkyl aromatic volatile products. The higher acidity of sulfated zirconia compared to the other catalysts results in an increase in the frequency of hydride abstractions, resulting in the formation of significant yields of saturated hydrocarbons and organic residue for this catalyst. Primary polypropylene cracking products can be derived from carbenium ion reaction mechanisms. © 1998 John Wiley & Sons, Inc. *J Appl Polym Sci* **67**: 341–348, 1998

Key words: polypropylene; polymer cracking; polymer recycling

INTRODUCTION

A variety of plastic waste recycling methods have been established and new recycling approaches are being developed to avoid placing polymers into landfills. One approach to waste plastic recycling, known as tertiary recycling, consists of converting plastics into useful chemicals. Large scale plastic waste tertiary recycling will require efficient and selective catalytic cracking of waste polymers. The development of waste polymer cracking processes will require detailed knowledge of the relationship between catalyst properties and cracking product distributions. In order to compare the polymer cracking properties of different catalysts, it is preferable to examine the effects of catalysts without complications due to reactions of primary cracking products with polymer residue. Secondary reactions can be minimized by limiting the contact between primary volatile products and the polymer–catalyst mixture. This can be accomplished by maintaining high catalyst-to-polymer

ratios and providing efficient and rapid removal of volatile products.^{1,2}

Several different catalysts have been used for catalytic cracking of polypropylene (PP). For example, activated carbon has been shown to catalytically crack PP.³ Activated carbon containing Pt and Fe was used to convert PP to aromatics in a fixed bed reactor.⁴ Silica–alumina and zeolite catalysts have also been employed to catalytically crack PP.^{5–8} However, because no attempts were made to eliminate secondary reactions in these studies, reported product distributions were not necessarily representative of initial volatile cracking products. To determine the relationship between acid catalyst properties and primary catalytic cracking products derived from PP, volatile products evolved during PP cracking by silica–alumina, HZSM-5, and sulfated zirconia under conditions that facilitated rapid removal of volatiles from polymer residues were compared. Sulfated zirconia was selected for study because it is a very strong acid catalyst.⁹ HZSM-5 acidity is somewhat higher than silica–alumina, but much lower than sulfated zirconia. In addition, HZSM-5 and silica–alumina catalysts differ in that HZSM-5 has well-defined channels, whereas silica–alumina is amorphous.

Correspondence to: R. L. White.

Journal of Applied Polymer Science, Vol. 67, 341–348 (1998)
© 1998 John Wiley & Sons, Inc. CCC 0021-8995/98/020341-08

EXPERIMENTAL

Samples used for this study were neat PP and PP mixed with silica–alumina (PP/SA), HZSM-5 (PP/MZ), and sulfated zirconia (PP/SZ) catalysts. Samples were prepared by mixing catalyst and polymer powders and were 10–15% PP by weight. Isotactic PP used in this study was purchased from Aldrich Chemical Company (Milwaukee, WI). Sulfated zirconia (SZ) was made by following procedures described in the literature¹⁰ and was calcined at 600°C prior to use. The silica–alumina catalyst was obtained from Condea Chemie GmbH (Hamburg, Germany). The silica–alumina catalyst contained 11.8%-by-weight alumina and had a surface area of 282 m²/g. The HZSM-5 zeolite catalyst was obtained from Mobil Oil (Paulsboro, NJ) and was characterized by a 355-m²/g surface area and a 1.5% alumina content.

TG-MS analyses were performed by interfacing a DuPont (Wilmington, DE) model 951 thermogravimetric analyzer and a Hewlett–Packard (Palo Alto, CA) 5985 quadrupole mass spectrometer. The interface contained a Scientific Glass Engineering Inc. (Austin TX) MCVT-1-50 variable splitter valve that was adjusted to achieve mass spectrometer ion source pressures in the range of 1×10^{-5} to 5×10^{-5} torr, depending on the TG heating rate employed. For TG-MS analyses, samples were heated from 50 to 600°C at nominal heating rates of 1, 10, 25, and 50°C/min with a He purge gas flow rate of 50 mL/min.

For TG-GC/MS measurements, a Valco Instruments (Houston, TX) $\frac{1}{16}$ -in. zero volume sampling valve was used to make injections of TG effluent into a capillary gas chromatograph. The TG-GC/MS apparatus is described in detail elsewhere.¹¹ TG effluent injections were made at three points along TG weight loss curves: between 20 and 30% conversion, between 40 and 60% conversion, and between 70 and 90% conversion. The three TG-GC/MS chromatograms were obtained from different samples taken from the same polymer/catalyst mixture. For TG-GC/MS analyses, the TG heating rate was adjusted to 30°C/min and TG He purge gas was added at a rate of 25 mL/min. TG-GC/MS signal averaged mass spectra were acquired at rates ranging from one to two per second, depending on the mass range that was scanned. The GC contained a 10-m DB-5 capillary column with a 0.25- μ m stationary phase film thickness. GC separations employed a 2-mL/min He carrier gas flow rate. The GC oven temperature program for TG-GC/MS analysis of neat PP

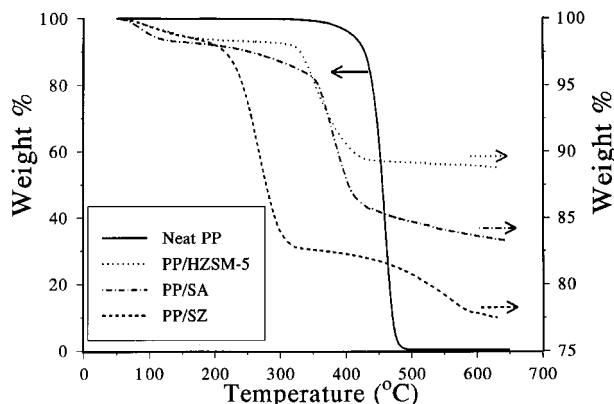


Figure 1 TG-MS weight loss curves for neat PP and PP/catalyst mixtures obtained by heating samples at 10°C/min.

and PP/SA samples consisted of a 2-min isothermal period at -50°C , a $5^{\circ}\text{C}/\text{min}$ ramp to 40°C , a $10^{\circ}\text{C}/\text{min}$ ramp to 250°C , and a 10-min isothermal period at 250°C . For TG-GC/MS analyses of PP/SZ samples, the temperature program began with a 2-min isothermal period at 5°C followed by a $10^{\circ}\text{C}/\text{min}$ ramp to 250°C and a 10-min isothermal period at 250°C . For TG-GC/MS analysis of PP/MZ samples, the temperature program consisted of a 2-min isothermal period at -20°C , a $10^{\circ}\text{C}/\text{min}$ ramp to 10°C , a $50^{\circ}\text{C}/\text{min}$ ramp to 260°C , and a 10 min isothermal period at 260°C . Samples of 30–65 mg were used for TG-GC/MS analyses. Separated species were identified with the aid of a 36,218 spectra NBS mass spectral library.

Thermooxidative TG analysis was used to measure the mass of carbonaceous residue remaining after polymer cracking by heating samples at $10^{\circ}\text{C}/\text{min}$ while purging with air at 15 mL/min.

RESULTS

Figure 1 shows TG-MS weight loss curves for neat PP and PP mixed with silica–alumina, HZSM-5, and sulfated zirconia catalysts. The left y -axis denotes weight percent for the neat PP sample and the right y -axis denotes weight percent for PP/catalyst samples. Neat PP thermally cracked above 400°C yielded no detectable residue. Mass spectra obtained for TG-MS effluent from neat PP samples contained many fragment ions, suggesting the presence of many different volatile species. Fragment ions with m/z values as large as 210 were detected. The most abundant ions were found at m/z 83, 69, and 55, which are rep-

representative of olefins. However, specific products could not be identified by TG-MS analysis alone.

Samples containing catalysts exhibited small TG-MS weight loss steps near 100°C (Fig. 1) that were attributed to water desorption based on the appearance of m/z 18 in mass spectra. The PP/SA and PP/MZ samples yielded volatile PP cracking products between 350 and 420°C, whereas volatile products produced by PP cracking for the PP/SZ sample were evolved below 300°C. Unlike neat PP thermal cracking, most volatile PP/catalyst cracking products detected by TG-MS yielded fragment ions with m/z values below 100. PP/SA sample TG-MS mass spectra contained fragment ions that were consistent with the formation of C₄ to C₆ olefins. PP/MZ sample TG-MS mass spectra contained fragment ions that were consistent with C₄ and C₅ olefins and m/z 91, which is indicative of alkyl aromatics. In contrast to the PP/SA and PP/MZ analysis results, TG-MS mass spectra obtained for PP/SZ samples contained fragment ions that were consistent with the evolution of saturated hydrocarbons. Unlike the PP/SA and PP/MZ samples, the PP/SZ sample exhibited a weight loss step between 500 to 600°C, corresponding to CO₂ and SO₂ evolution that resulted from catalyst decomposition. Similar sulfated zirconia catalyst decompositions were previously reported in this temperature range when polyethylene and polystyrene were cracked by this catalyst.^{1,2}

The amount of char remaining on catalyst surfaces after PP cracking in He was measured by thermooxidative TG analysis. For the PP/SA and PP/MZ samples, the mass of oxidizable residue was found to be below the detection limit of the TG analyzer, which was estimated to be ~ 1% of the initial polymer mass. Other researchers also reported little residue after PP catalytic cracking with these types of catalysts.^{5,6} In contrast, ~ 15% of the PP/SZ initial polymer weight remained as char after catalytic cracking in He.

TG-GC/MS total ion current (TIC) chromatograms for neat PP thermal decomposition products obtained at 20, 50, and 80% conversion are shown in Figure 2. The most abundant volatile products detected at all three conversions were the same and are listed by carbon number in Table I. Entries in Table I correspond to percentages of TG-GC/MS chromatogram integrated total ion currents attributed to chromatographic elutions for all isomeric species having the same numbers of carbons and hydrogens. The most abundant neat PP thermal cracking volatile products were C₃–C₁₅ olefin homologs separated by three carbon atom intervals. The most abundant saturated

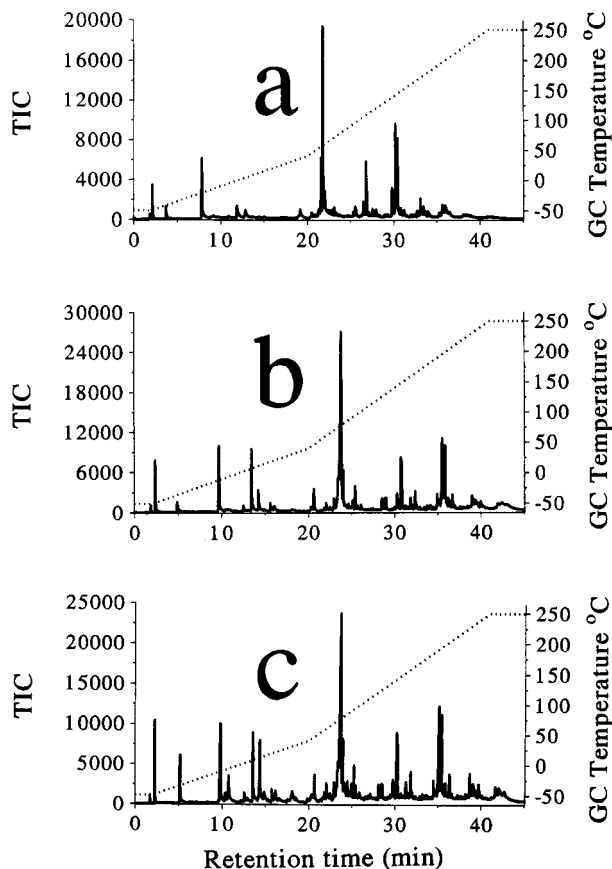


Figure 2 TG-GC/MS chromatograms obtained by injecting neat PP TG effluent at (a) 20%, (b) 50%, and (c) 80% PP conversions.

volatile products were C₅H₁₂ species. The primary volatile products listed in Table I are consistent with those previously reported for neat PP thermal decompositions and can be derived from free radical mechanisms involving β -scissions of tertiary chain radicals.^{12–14}

Catalytic cracking of PP/SA samples produced a significantly different volatile product distribution than neat PP thermal cracking. As shown in Figure 3, all of the volatile products detected by TG-GC/MS analysis of the PP/SA sample eluted in less than 17 min when the same chromatographic conditions employed for neat PP analyses were used for separations. In contrast to neat PP thermal cracking, the most abundant volatile products derived from PP/SA catalytic cracking were C₄H₈, C₅H₁₀, and C₆H₁₂ species (Table II). Relative yields for volatile hydrocarbons larger than C₆ increased as percent conversion increased. Volatile product distributions in Table II are consistent with previously published results in which silica–alumina was used to crack PP.^{5,15}

TG-GC/MS total ion current chromatograms

Table I TG-GC/MS Volatile Product Yields for Neat PP

Cracking Products	Retention Time (min)	20% Conversion	50% Conversion	80% Conversion
C ₂ H ₆	1.7–1.9	0.3 ^a	0.2	0.2
C ₃ H ₆	2.1–2.5	2.4	2.7	2.7
C ₄ H ₈	3.7–5.1	1.4	1.3	3.1
C ₅ H ₁₂	7.8–9.8	7.2	6.1	5.7
C ₅ H ₁₀	9.1–10.9	0.9	0.7	2.7
C ₆ H ₁₄	10.9–12.5	0.6	0.6	0.5
C ₆ H ₁₂	11.5–14.9	5.8	6.4	8.6
C ₇ H ₁₄	14.4–18.5	1.5	1.2	3.2
C ₈ H ₁₈	19.2–20.6	2.5	1.5	1.1
C ₈ H ₁₆	19.8–22.6		0.8	2.6
C ₉ H ₁₈	20.5–25.6	35	41	34
C ₁₀ H ₂₀	25.0–27.5	0.5	1.9	2.9
C ₁₁ H ₂₄	25.5–29.0	1.2	0.9	0.7
C ₁₁ H ₂₂	25.3–28.5	0.6	0.6	0.7
C ₁₂ H ₂₄	26.4–30.8	6.3	5.9	5.0
C ₁₅ H ₃₀	29.7–36.7	16	16	12

^a Percentage of integrated total ion current from TG-GC/MS chromatograms.

obtained for PP/SZ samples are shown in Figure 4. In contrast to the neat PP and PP/SA samples, the most abundant cracking products for PP/SZ samples were saturated hydrocarbons (Table III). All of the volatile hydrocarbons detected by TG-GC/MS were C₁₀ or smaller. Whereas the TG-GC/MS total ion current chromatograms obtained at 21 and 43% conversion were similar, the chromatogram obtained at 83% conversion exhibited a significant increase in unsaturated volatile product yields compared to those obtained at lower conversions.

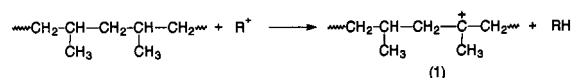
Figure 5 shows that volatile cracking products for PP/MZ samples were also dependent on PP conversion. Table IV reveals that at 27% conversion, most volatile products were hydrocarbons with retention times of < 4 min. These results are consistent with previous reports of PP catalytic cracking with zeolites.^{5,15–18} In contrast to the chromatogram obtained for volatile products generated at 27% conversion, chromatograms obtained at 55 and 76% conversion exhibited increased abundance for alkyl aromatic species eluting between 7 and 9 min.

DISCUSSION

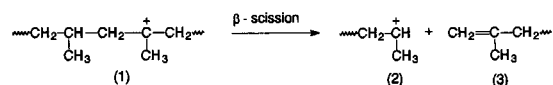
PP/SA Cracking

The most abundant volatile products formed by cracking PP with silica–alumina catalyst were C₄–C₆ olefins. Formation of these products can

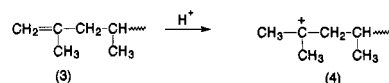
be explained by carbenium ion reaction mechanisms.^{5,6,16,17} Initial formation of carbenium ions has been proposed to occur from trace impurities or polymer weak links by protonation or hydride abstraction.⁷ After initial formation of carbenium ions, tertiary carbenium ions can readily be formed by hydride abstraction at polymer backbone sites where methyl groups are attached.



Because of the greater stability of tertiary carbenium ions, rearrangements from primary and secondary ions to tertiary ions would be favored. β -scission of **1** would produce a secondary carbenium ion (**2**) and a chain end olefin (**3**).



The chain end olefin could readily undergo electrophilic attack by a proton to produce a chain end tertiary carbenium ion (**4**).



β -scission of this chain end tertiary ion would produce isobutene (C₄H₈) and a secondary carbenium ion. TG-GC/MS results obtained for all PP/cata-

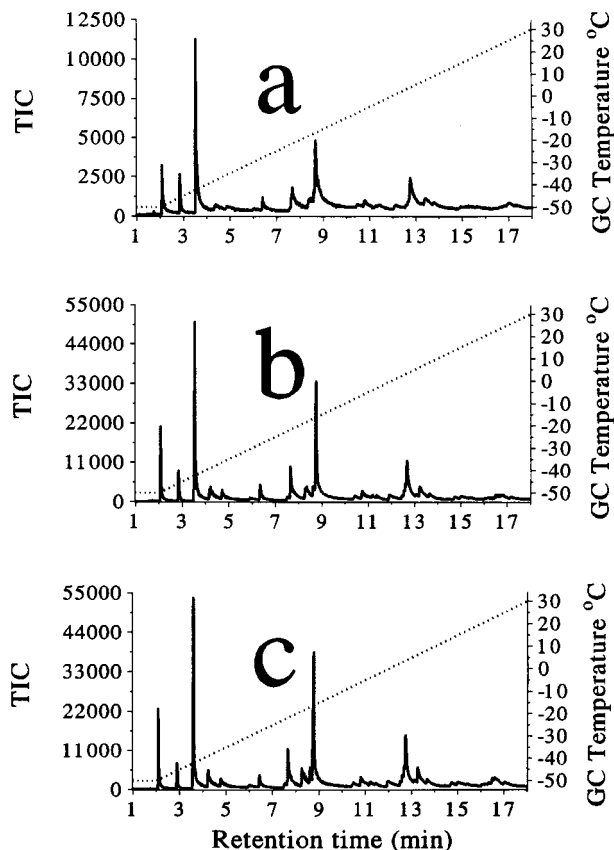
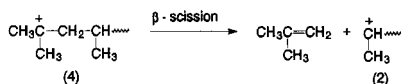


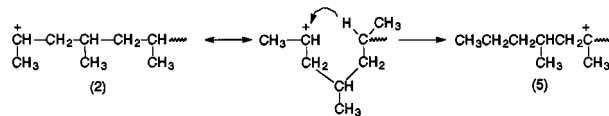
Figure 3 TG-GC/MS chromatograms obtained by injecting PP/SA TG effluent at (a) 24%, (b) 58%, and (c) 75% PP conversions.

lyst samples confirmed that the most abundant butene isomer was indeed isobutene.

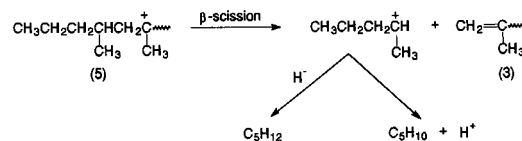


Unsaturated C_5 species can be derived from secondary carbenium ions after intramolecular rear-

rangements to form more stable tertiary carbenium ions (5).



β -scissions of 5 can produce unsaturated chain ends (3) and C_5 carbenium ions. C_5 carbenium ions can abstract hydrides to form saturated hydrocarbon products or lose a proton to form C_5 olefins. The electron-rich chain end olefin formed by 5 β -scission would be a convenient target for protonation by the C_5 carbenium ion.



The large yield of C_5 olefins (Table II) suggests that the latter route was a dominant reaction pathway when PP was cracked by silica–alumina. Branched C_5 products would be formed if the C_5 carbenium ion rearranged prior to hydride abstraction or loss of a proton. Results from TG-GC/MS analyses suggest that C_5 carbenium ion rearrangement readily occurred on all three catalysts because 2-methylbutane was the only saturated C_5 volatile product detected. One C_5 olefin was detected by TG-GC/MS analysis of the PP/SZ sample. Two C_5 olefin isomers were detected by TG-GC/MS analyses of PP/SA and PP/MZ samples. Mass spectra for these C_5 species were very similar and library searches indicated that they were either 2-pentene or branched olefins, which also suggests that C_5 carbenium ion rearrangements readily occurred.

Table II TG-GC/MS Volatile Product Yields for PP/SA

Cracking Products	Retention Time (min)	24% Conversion	58% Conversion	75% Conversion
C_3H_6	2.1–2.3	5.8 ^a	6.0	4.7
C_4H_8	3.5–5.0	24	25	21
C_5H_{10}	7.5–9.5	36	34	31
C_6H_{12}	12.0–14.0	16	17	21
C_4H_{10}	2.8–3.0	3.0	2.9	1.8
C_5H_{12}	6.3–6.6	2.2	2.4	1.5
C_6H_{14}	10.3–11.7	4.0	3.5	3.1
$>\text{C}_6$	>12	8.1	9.4	16

^a Percentage of integrated total ion current from TG-GC/MS chromatograms.

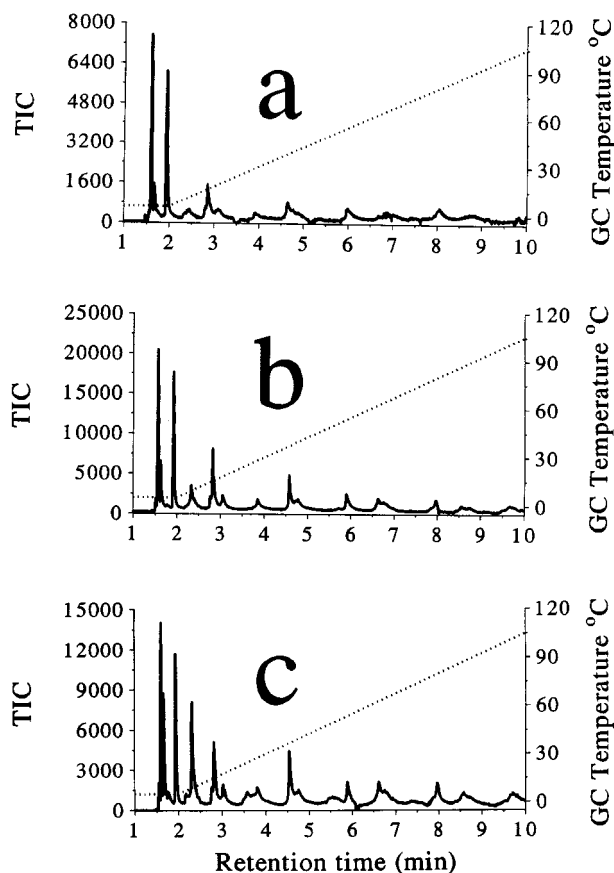
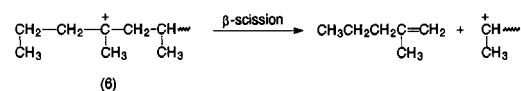


Figure 4 TG-GC/MS chromatograms obtained by injecting PP/SZ TG effluent at (a) 21%, (b) 43%, and (c) 83% PP conversions.

C_6 olefins can be formed by β -scission of tertiary carbenium ions located near the ends of polymer chains (**6**).



The increase in the relative yield of C_6 olefins with increasing conversion for PP/SA samples (Table II) may have resulted from polymer chain shortening with increasing conversion, which would increase the probability of forming chain end tertiary carbenium ions (**6**).

PP/SZ Cracking

In contrast to the PP/SA cracking product distributions, the most abundant cracking products generated by cracking PP with sulfated zirconia were saturated hydrocarbons (Table III). This is consistent with results from our recent study of the reactions of 1-butene on sulfated zirconia.¹⁹ Due to the high acidity of the sulfated zirconia catalyst, surface interactions between carbenium ions and conjugate base catalyst sites are weak. As a result, carbenium ions are stronger Lewis acids than those formed on weaker acid catalysts. Thus, carbenium ions on sulfated zirconia are more likely to abstract hydrides than those on silica–alumina or HZSM-5 catalysts. This resulted in the increased abundance of volatile saturated hydrocarbon products produced when sulfated zirconia was used as the catalyst. The increase in the rate of hydride abstractions during PP/SZ cracking was also responsible for the much larger quantities of residue remaining after cracking on sulfated zirconia catalyst surfaces than on

Table III TG-GC/MS Volatile Product Yields for PP/SZ

Cracking Products	Retention Time (min)	21% Conversion	43% Conversion	83% Conversion
C_3H_6	1.50–1.55	0.4 ^a	0.8	1.0
C_4H_{10}	1.55–1.60	19	15	9.2
C_4H_8	1.6–1.8	4.1	4.9	6.7
C_5H_{12}	1.9–2.0	19	16	9.1
C_5H_{10}	2.1–2.4	4.1	5.5	9.1
C_6H_{14}	2.7–3.1	12	8.9	7.0
C_6H_{12}	3.6–3.8	—	—	5.2
C_7H_{14} and C_7H_{16}	3.8–5.6	11	13	10
C_8H_{18}	5.9–6.9	10	13	11
C_8H_{16}	6.6–7.5	—	—	2.1
C_9H_{20}	8.0–8.8	8.4	9.3	4.1
C_9H_{18}	8.6	—	—	4.2
$C_{10}H_{22}$ and $C_{10}H_{24}$	9.8–10.5	—	9.3	9.0

^a Percentage of integrated total ion current from TG-GC/MS chromatograms.

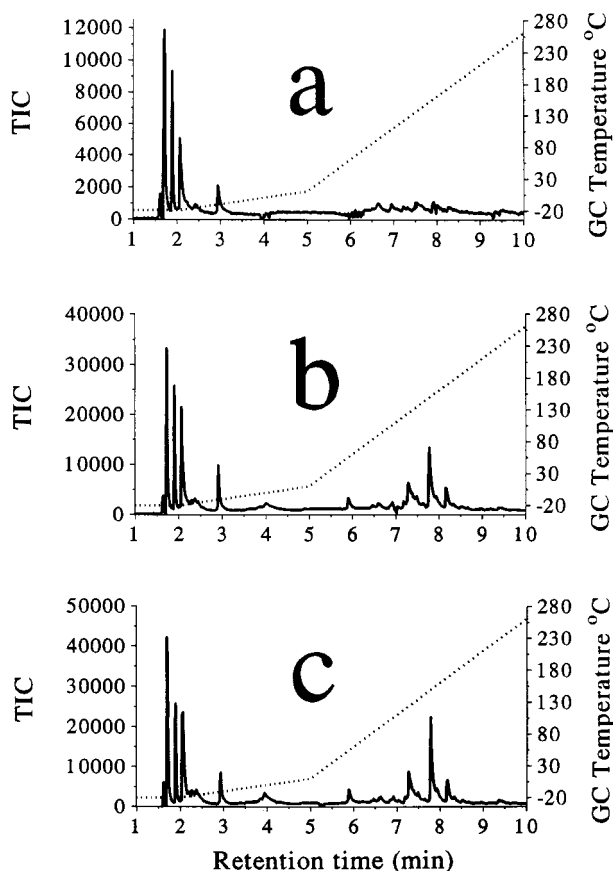


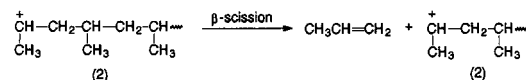
Figure 5 TG-GC/MS chromatograms obtained by injecting PP/MZ TG effluent at (a) 27%, (b) 55%, and (c) 76% PP conversions.

silica–alumina or HZSM-5 catalysts. The increase in unsaturated product yields detected at 83% conversion (Table III) likely resulted from

partial decomposition of the unsaturated residue formed by extensive hydride abstractions.

PP/MZ Cracking

The most abundant volatile product derived from the PP/MZ sample at 27% conversion was propene. Propene can be formed by β -scission of secondary chain-end carbenium ions.



However, rearrangement of these ions to tertiary carbenium ions is reportedly more thermodynamically favored than β -scission.⁶ In fact, the preference for rearrangement of this carbenium ion was likely the reason that C₅ olefin yields were much larger than propene yields for the PP/SA and PP/SZ samples (Tables II and III). In contrast to results obtained for PP/SA and PP/SZ samples, C₅ olefins were not detected at 27% conversion for the PP/MZ sample. This was likely due to the difficulty of forming the six-membered ring intermediate inside HZSM-5 channels that is required to produce **5**. Table IV also shows that propene yield decreased with increasing conversion for the PP/MZ sample. Interestingly, the yields of alkyl aromatics increased with increasing conversion. It appears that alkyl aromatics were formed at the expense of propene production. Propene formed within HZSM-5 channels likely participated in oligomerization reactions to form alkyl aromatics.²⁰ The size range of volatile alkyl aromatics

Table IV TG-GC/MS Volatile Product Yields for PP/MZ

Cracking Products	Retention Time (min)	27% Conversion	55% Conversion	76% Conversion
C ₂ H ₄	1.6–1.7	2.5 ^a	1.6	2.0
C ₃ H ₆	1.7–1.8	31	17	19
C ₄ H ₁₀	1.9–2.0	18	11	11
C ₄ H ₈	2.0–2.4	18	17	22
C ₅ H ₁₂	2.8–3.0	6.0	6.6	4.4
C ₅ H ₁₀	3.9–4.0	—	6.4	4.9
C ₆ , C ₇ , and C ₈	5.8–7.7	11	7.1	7.5
C ₇ H ₈ ^b	7.2–7.4	4.5	11	6.0
C ₈ H ₁₀ ^b	7.8–7.9	4.8	16	17
C ₉ H ₁₂ ^b	8.1–8.4	2.5	4.6	4.0
C ₁₀ H ₁₄ ^b	8.4–8.7	—	0.4	0.4
C ₁₁ H ₁₀ ^b	9.3–9.5	1.2	0.8	1.1

^a Percentage of integrated total ion current from TG-GC/MS chromatograms.

^b Aromatic products.

that could be formed was limited to C₁₁ by volume restrictions imposed by the zeolite channel structure.

CONCLUSIONS

The fact that volatile PP cracking products are significantly different when silica–alumina and sulfated zirconia are employed as cracking catalysts suggests that catalyst acidity is an important factor in determining volatile product slates. Sulfated zirconia, which is a very strong acid catalyst, significantly lowered the temperature at which catalytic cracking occurred and facilitated hydride abstractions, resulting in large yields of saturated hydrocarbon products and the formation of large amounts of oxidizable organic residue. In contrast, the primary volatile products derived by using silica–alumina and HZSM-5 as cracking catalysts were olefins. Compared to sulfated zirconia, PP catalytic cracking required higher temperatures for the silica–alumina and HZSM-5 catalysts, which were weaker acids than sulfated zirconia. Comparing results obtained from PP cracking with silica–alumina and HZSM-5 catalysts, the restricted reaction volume afforded by HZSM-5 inhibited the reaction pathway for formation of C₅ olefins and enhanced the yield of propene. In addition, alkyl aromatics, which were not detected as volatile products when PP was cracked by silica–alumina, were formed in relatively large yields inside HZSM-5 channels.

Financial support for this work from the National Science Foundation (CTS-9509240) is gratefully acknowledged.

REFERENCES

1. R. Lin and R. L. White, *J. Appl. Polym. Sci.*, **58**, 1151 (1995).
2. R. Lin and R. L. White, *J. Appl. Polym. Sci.*, **63**, 1287 (1997).
3. Y. Uemichi, A. Ayame, N. Noguchi, and H. Kanoh, *Nippon Kagaku Kaishi*, 1429 (1985).
4. Y. Uemichi, Y. Makino, and T. Kanazuka, *J. Anal. Appl. Pyr.*, **16**, 229 (1989).
5. G. Audisio and A. Silvani, *J. Anal. Appl. Pyr.*, **7**, 83 (1984).
6. Y. Ishihara, H. Nanbu, K. Saido, T. Ikemura, T. Takesue, and T. Kuroki, *Fuel*, **72**, 8, 1115 (1993).
7. Y. Ishihara, H. Nanbu, C. Iwata, T. Ikemura, and T. Takesue, *Bull. Chem. Soc. Jpn.*, **62**, 2981 (1989).
8. Y. Sakata, M. Uddin, K. Koizumi, and K. Murata, *Chem. Lett.*, **3**, 245 (1996).
9. T. Okuhara, T. Nishimura, H. Watanabe, and M. Misono, *J. Mol. Catal.*, **74**, 247 (1992).
10. A. Jatia, C. Chang, J. D. MacLeod, T. Okube, and M. E. Davis, *Catal. Lett.*, **25**, 21 (1994).
11. E. C. Sikabwe, D. L. Negelein, R. Lin and R. L. White, *Anal. Chem.*, **69**, 2606 (1997).
12. Y. Tsuchiya and K. Sumi, *J. Polym. Sci. A-1*, **7**, 1599 (1969).
13. E. Kiran and J. K. Gillham, *J. Appl. Polym. Sci.*, **20**, 2045 (1976).
14. V. J. Triacca, P. E. Gloor, S. Zhu, A. N. Hrymak, and A. E. Hamielec, *Polym. Eng. Sci.*, **33**, 445 (1993).
15. Y. Uemichi, Y. Kashiwaya, M. Tsukidate, A. Ayame, and H. Kanoh, *Bull. Chem. Soc. Jpn.*, **56**, 2768 (1983).
16. W. Zhao, S. Hasegawa, J. Fujita, F. Yoshii, T. Sasaki, K. Makuuchi, J. Sun, and S. Nishimoto, *Polym. Degrad. Stab.*, **53**, 129 (1996).
17. I. Kodaira, Z. Osawa, and H. Ando, *Nippon Kagaku Kaishi*, 1892 (1977).
18. R. C. Mordi, R. Fields, and J. Dwyer, *J. Chem. Soc. Chem. Commun.*, 374 (1992).
19. E. C. Sikabwe and R. L. White, *Catal. Lett.*, **44**, 177 (1997).
20. P. Magnoux, P. Roger, C. Canaff, V. Fouche, N. S. Gnep, and M. Guisnet, *Stud. Surf. Sci. Catal.*, **34**, 317 (1987).